Selective remote excitation of complex structures using time reversal in audible frequency range

Maxime Farin,[a] Claire Prada, and Julien de Rosny

*Ecole Supérieure de Physique et de Chimie de la ville de Paris, Paris Sciences et Lettres Research University,
Centre National de la Recherche Scientifique, Institut Langevin, 1 rue Jussieu, Paris, France*

Generation of elastic waves is a major issue in nondestructive testing. Structural health monitoring of a thin element can be achieved through the analysis of its resonance spectrum. A time reversal mirror (TRM) operating in the audible frequency range (1–10 kHz) is used to remotely excite thin resonant elastic elements. The generation of elastic waves is studied with respect to the geometry of the TRM. It is observed that the quality of focusing only weakly depends on the number of loudspeakers (LS) in the TRM. When the air/plate coupling is at its maximum, the energetic efficiency of the TRM is estimated to be about 0.02%. The TRM is shown to efficiently and selectively excite a small structure embedded in a complex environment such as a hollow cylinder. Finally, the results are discussed in light of the DORT method (French acronym for "decomposition of the time reversal operator"). In particular, the optimal LS placement and emission signals in this configuration to excite individual eigenmodes of a plate is determined. © *2019 Acoustical Society of America*.
https://doi.org/10.1121/1.5129130

I. INTRODUCTION

Many industrial applications (e.g., food-processing, automobile, aeronautic) use thin plates, shells, or pipes that need to be inspected regularly. Rapid detection and localization of defects, such as cracks, holes, or loose screws in a structure, is a huge issue for safety and machine optimal operating conditions. Verification of the structure integrity is usually performed through visual inspection (e.g., dye penetrant testing) or using vibrating piezoelectric transducers and accelerometers in contact with the structure (see Diamanti and Soutis, 2010; Rivière *et al*., 2010, for review). However, due to the complexity of industrial machines, numerous elements need to be inspected and are often difficult to access (e.g., storage tanks, gas and fluid pipes, blades in airplane turbine reactors, etc.), requiring operators to disassemble parts or the totality of the machine, which is time- and money-consuming. In this context, we would like to propose an experimental setup to conduct a rapid, remote, and selective excitation of a thin solid inside a complex structure in order to excite its resonance frequencies. All these requirements are feasible with a time reversal mirror (TRM). Such a system is used to focus sound energy at a specific location in space and time (see Fink *et al*., 2000, for a review of seminal works). A time reversal (TR) experiment is achieved in two steps. During the forward step, a wave emitted by an acoustic source propagates through the medium and is recorded by a set of transducers. During the backward step, the recorded signals are flipped in time and re-emitted by the transducers. The emitted sound wave then follows the initial path of the wavefront in the opposite direction, and focuses as an impulse at the initial source position as if time was

flowing backward. TRMs have been applied to achieve focusing in different contexts either in water (Prada *et al*., 1996; Kuperman *et al*., 1998) or air (Ribay *et al*., 2005; Yon *et al*., 2003), or to detect and image linear defects (Chakroun *et al*., 1995) or non-linear defects (see Anderson *et al*., 2019, for review) in solids. An important advantage of the TR process is that it does not require *a priori* knowledge of the structure geometry. Indeed, if the experiment is conducted in a reverberant cavity (e.g., a small room) or in the presence of scatterers between the array of transducers and the source, contrary to classical beamforming processing, TR still generates converging waves (Derode *et al*., 1995; Draeger and Fink, 1997; Yon *et al*., 2003). Even more, it has been shown that the focusing is improved because the obstacles or the cavity boundaries act as virtual TR elements. Additionally, if a source is not available at the targeted focusing position, the impulse responses from the source to the TR transducers can be advantageously replaced by the impulse responses from the TR transducers to the desired focusing position. Indeed in a reciprocal media, those responses are equal (Draeger *et al*., 1998a) and taking advantage of this property is particularly interesting to inspect objects that are difficult to access.

Here, our objective is to remotely and selectively excite a thin plate using a TRM placed in air. Practically, this consists in focusing the flexural waves in the plate using a non-contact acoustic source. In 1998, Ing and Fink (1998) demonstrated the focusing of flexural waves in thin plates using a laser excitation and piezoelectric transducers in contact with the plate. Recently, Payan *et al*. (2017) were able to locally focus either symmetrical S_0 or anti-symmetrical A_0 Lamb modes in a plate of non-uniform thickness. To excite a plate with sound involves mode conversion from acoustic waves into flexural waves. Besides its focusing property, the TR process also ensures that back conversion occurs

[a])Electronic mail: maxime.farin@espci.fr

(Draeger *et al.*, 1998b). Combining this effect with the use of a single or a few transducers attached to a reverberating elastic cavity, several studies showed that acoustic waves are efficiently focused either in water (Montaldo *et al.*, 2001; Quieffin *et al.*, 2004), air (Etaix *et al.*, 2012; Etaix *et al.*, 2013), or solids (Van Den Abeele *et al.*, 2010). More recently, Le Bas *et al.* (2013) and Le Bas *et al.* (2015) reported that non-contact local excitation on a plate is possible using an ultrasonic source in air (see also Anderson *et al.*, 2019, for a review). To this end, they built a TRM composed of piezoelectric transducers inside a hollow closed cavity with an opening located at a fixed distance 2 cm in front of the plate. Plate vibration was recorded using a laser vibrometer. The focal spots are recorded at various positions by moving the TRM along the plate in order to locate millimeter-size delamination. Here, we propose a different but complementary approach. The TRM is made of an array of loudspeakers (LS) working in the audible frequency range (1–10 kHz) to selectively excite a resonant object located a few meters away. Excitation from this distance allows a fast and global test of the whole object from a fixed position of the TRM. The idea is to conduct an evaluation of the object resonance frequency spectrum by focusing flexural waves at a single position because it is known that a defect occurrence induces a shift of the resonance frequencies (Salawu, 1997). This procedure is especially interesting in the case of several objects embedded in a complex structure. While being unable to locate the defect, the proposed method is much faster than those requiring a systematic scan of the object. After presenting the experimental setup to excite a thin duralumin plate, we investigate the conditions on the LS array arrangement and frequency content of the emitted signal for which the amplitude and contrast of the plate excitation are the best. We show that our TR technique allows us to excite selectively different thin plates placed in a complex structure. Finally, we analyze the property of focusing in such resonant media using the formalism of the TR operator and discuss the influence of room reverberation on the TR process.

II. EXPERIMENTAL SETUP AND FOCUSING PROCESS

The TRM is composed of an array of LS. Each loudspeaker consists in a mini multimedia loudspeaker (Ryght™, Paris) with a diameter of 6 cm. 32 LS are set in a rectangular 8×4 array of 20 cm pitch [Fig. 1(a)]. Each set of eight LS is connected to an electronic board developed at the laboratory to amplify the signals. A 32-channel analog-to-digital/digital-to-analog (AD/DA) converter (Orion 32 channels, Antelope, Elecktrosfera Ltd, Sofia, Bulgaria) with a resolution of 24 bits samples data at a rate of 96 kS/s. The data are directly transferred to a computer via a high-speed Universal Serial Bus (USB) connection resulting in a latency as small as a few milliseconds. To manage the 32 AD/DA channels, we use the PyAudio Python module.

Two types of plates are investigated: (1) a "large" 3-mm-thick duralumin plate of dimensions 60 cm per 50 cm and (2) a "small" 1-mm-thick duralumin plate of dimensions 10 cm per 10 cm. Duralumin has a density of 2700 kg m^{-3}, its Young modulus is 70 GPa, and its Poisson ratio is 0.35. In the frequency range of interest (1–10 kHz), most of the vibration energy of these plates is carried by the fundamental Lamb mode A_0. In this low-frequency regime, the highly dispersive A_0 mode is also called the flexural mode and is dominated by normal displacements (Royer and Dieulesaint, 2000). Therefore, the vibration of the plate can be fully measured using a one-dimensional sensor. Unless otherwise specified, the plate vibration is measured using a laser vibrometer (Polytec OFV-505, Waldbronn, Germany).

A. Forward step

The forward step of the TR focusing consists in recording the impulse responses $k_i(t)$ between the LS located at $\mathbf{r_i}$ and a point $\mathbf{r_0}$ on the targeted thin plate. To improve the signal-to-noise ratio, a linear frequency modulated (LFM) signal is emitted instead of a pulse. The impulse responses over the frequency range 1–10 kHz are extracted by correlating the received signal with the emitted LFM [Fig. 2(a)]. This step is repeated with each loudspeaker to obtain the set of responses $k_i(t)$ with $1 \leq i \leq 32$ [Figs. 1(a) and 1(b)].

B. Backward step

The second step takes advantage of the reciprocity of wave propagation. To focus back the flexural waves in the plate at the point $\mathbf{r_0}$, the responses $k_i(t)$ are flipped in time and re-emitted synchronously by all LS [Fig. 1(c)]. The emitted acoustic waves are converted back into flexural waves at the plate interface, forming a temporal impulse [Figs. 2(b) and 2(c)] and a focal spot around the focal position $\mathbf{r_0} = (x = 0, y = 0)$ [Fig. 2(e)]. Using all 32 LS emitting a 1-s signal successively in the forward step and a 1-s signal simultaneously in the backward step, the whole TR experiment lasts about 40 s. Neither repetition nor averaging of the focusing impulse are needed to measure the plate response with a good signal-to-noise ratio [Fig. 2(d)]. Note that, due to the limited dimensions of the plates, the eigenfrequencies of the plate are clearly distinguishable from each other on the spectrum. Similarly to the work performed with a single channel TR in a silicon cavity (Draeger and Fink, 1997), the focusing can be interpreted as the result of the constructive interference of the eigenmodes of the structure. However, here, and contrary to Draeger and Fink (1997), the TRM is not in contact with the plate. The amplitude ratio of the focal spot to secondary lobes can be evaluated by computing the point spread function (PSF)

$$\text{PSF}(x, y) = 20 \log_{10} \left(\frac{v_z(x, y, T)}{v_z(x = 0, y = 0, T)} \right). \quad (1)$$

In this experiment, the amplitude of the focal spot is about 10 dB higher than the secondary lobes, and the diameter of the spot is about 2 cm [Fig. 2(f)]. The effect of frequency on focusing quality is discussed in Sec. III.

III. EFFICIENT FOCUSING CONDITIONS

We describe here the influence of the number and locations of the TRM LS and frequency band on the quality of the focusing on a large duralumin plate.

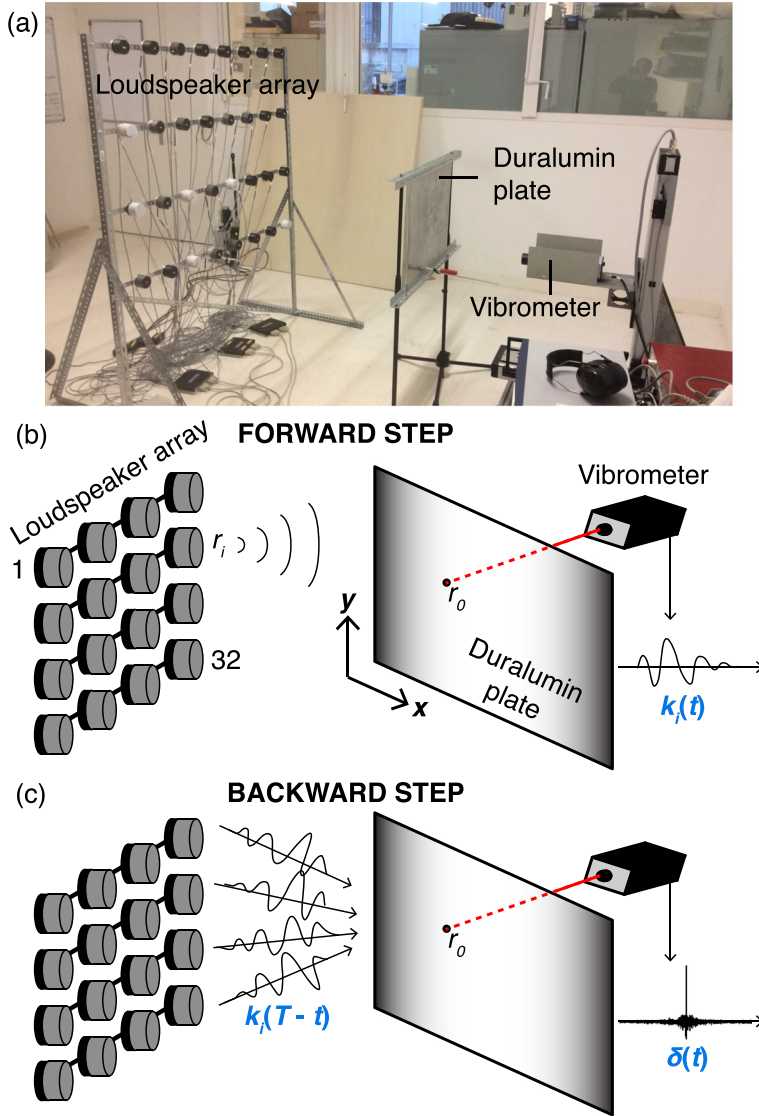J. Acoust. Soc. Am. **146** (4), October 2019

Farin *et al.* 2511

FIG. 1. (Color online) (a) Array of LS used as elements of the TRM to excite the eigenmodes of a duralumin plate and vibrometer used to measure the plate vibration. Schematic of the experiment: (b) Forward step: the impulse responses $k_i(t)$ between each loudspeaker in $\mathbf{r_i}$ and a point $\mathbf{r_0}$ on the plate are recorded with the laser vibrometer. (c) Backward step: all impulse responses are time reversed $[k_i(T-t)]$ and played simultaneously, and an impulse is measured at point $\mathbf{r_0}$.

A. Influence of number and location of LS

In order to test the influence of the number of LS and location on focusing, the 32 LS are arranged around the plate [Fig. 3(a)]. In this specific experiment, we do not use the laser vibrometer to measure impulse responses between the TRM and the plate. During the forward step, each loudspeaker emits successively. The impulse responses between all LS and one transducer are estimated from the recording by this last. The responses are flipped in time and sent back by the loudspeaker array during the backward step. Due to the TR invariance, an impulse is focused on the transducer. The plate vibration is simultaneously measured with five other transducers located at various distances from the transducer on which the field is focused. For a given arrangement of the LS with respect to the plate (normal or parallel), we observe on Fig. 3(b) that the peak focal amplitude increases with the number of LS. The increase is not linear as the amplitude at the focus is only 4 times larger when the number of LS goes from 2 to 32. This is because the coupling of a LS with the plate strongly depends on its position. This is further discussed in Sec. V. The PSF is plotted in Fig. 3(c). We observe that the

lowest level of secondary lobes is obtained when the LS distribution is parallel to the plate, i.e., when a strong coupling between the acoustic and elastic wave occurs. For the same reason, the PSF generated by two efficiently positioned LS can be as good as the PSF obtained with 32 LS positioned all around the plate. In the following, we place all 32 LS in the most efficient configuration, i.e., in a plane parallel to the plate surface, as shown in Fig. 1(a).

B. Influence of the excitation frequency

We now observe how the central frequency f_{mean} and bandwidth Δf of the signal emitted during the forward step [and therefore of the impulse response $k(t)$] affect the excitation amplitude and level of the secondary lobes. For a fixed bandwidth $\Delta f = 1\,\mathrm{kHz}$, the maximum plate excitation amplitude is higher when the central frequency f_{mean} is close to $4\,\mathrm{kHz}$ [Fig. 4(a)]. This corresponds to the critical frequency for which the acoustic wavelength λ_{air} equals that of the flexural mode within the plate $\lambda_{\mathrm{flexural}}$ (Fig. 5). This is in agreement with the fact that the radiation efficiency of thin plates (i.e., plate coupling with surrounding air) is maximum when
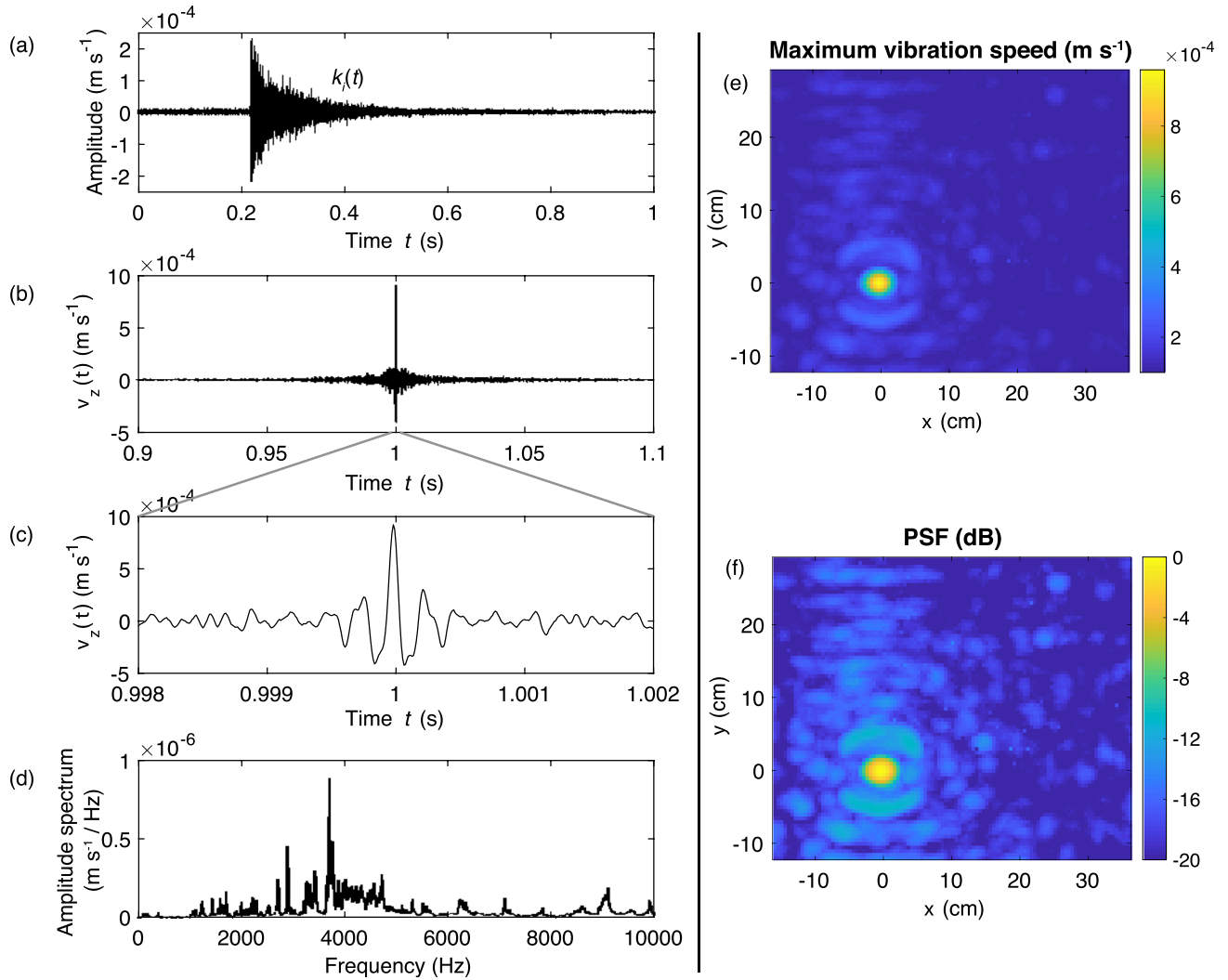
FIG. 2. (Color online) (a) Impulse response $k_i(t)$ measured with the vibrometer on the large duralumin plate with the setup shown in Fig. 1(a) with all 32 LS arranged in a array whose plane is parallel to the surface of the plate and emitting a signal (chirp) with bandwidth between 1 and 10 kHz. (b) Vibration speed $v_z(t)$ at the focal location $\mathbf{r_0}$. (c) Enlargement of $v_z(t)$ around focusing time. (d) Amplitude spectrum $|\tilde{V}_z(f)|$ of the impulse signal $v_z(t)$. (e) Maximum amplitude of vibration speed $v_z(t)$, and (f) point spread function (PSF) on the large duralumin plate. The focal spot is at $(x=0, y=0)$.

λ_{air} is close to $\lambda_{\text{flexural}}$ (Filippi, 2010; Wallace, 1972). Related to this, we note in Fig. 4(b) that the width of the focal spot is determined by half a wavelength $\lambda_{\text{air}}/2$ and, consequently, decreases when the frequency f_{mean} increases (Le Bas *et al.*, 2015; Yon *et al.*, 2003).

For a given central frequency $f_{\text{mean}} = 4\,\text{kHz}$, the maximum plate excitation amplitude increases and the level of the secondary lobes decreases as the signal bandwidth Δf increases [Figs. 4(c) and 4(d)]. This is due to the fact that the amplitudes of the plate eigenmodes sum constructively at the focal position $\mathbf{r_0}$ and destructively elsewhere. Indeed, when more eigenmodes are excited by increasing signal bandwidth, the focal spot has a higher amplitude and is more clearly visible. In contrast, for a short bandwidth $\Delta f = 100\,\text{Hz}$ around $f_{\text{mean}} = 4\,\text{kHz}$, we mainly excite one single mode of the plate, and the focal spot is not clearly distinguishable from an antinode of the eigenmode [Fig. 4(d)]. In the following, signals of frequencies 1–10 kHz are emitted to enhance the absolute plate excitation amplitude and focal spot/secondary lobes amplitude ratio.

IV. SELECTIVE FOCUSING INSIDE A COMPLEX STRUCTURE

In Sec. II, we have determined a configuration for which the remote excitation of a plate is efficient when no obstacles are present between the TRM and targeted plate. In this section, we propose to test the technique on a plate placed inside a complex structure.

A. Excitation of a plate inside a tube

In order to investigate the effect on the plate excitation of the presence of a complex structure around the plate, we conduct two experiments. First, we excite a square 1-mm-thick duralumin plate placed at ~1 m in front of the LS, with no obstacles between it and the LS array [Fig. 6a]. Then, we excite the same plate placed at the exact same position but inside a stainless steel tube of length 2 m, diameter 20 cm, and thickness 1 mm [Fig. 6(b)]. In both cases, the same plate eigenmodes are excited and the focal spot is unchanged [Figs. 6(c)–6(g)]. However, the efficiency of the focusing (i.e., ratio of elastic

J. Acoust. Soc. Am. **146** (4), October 2019
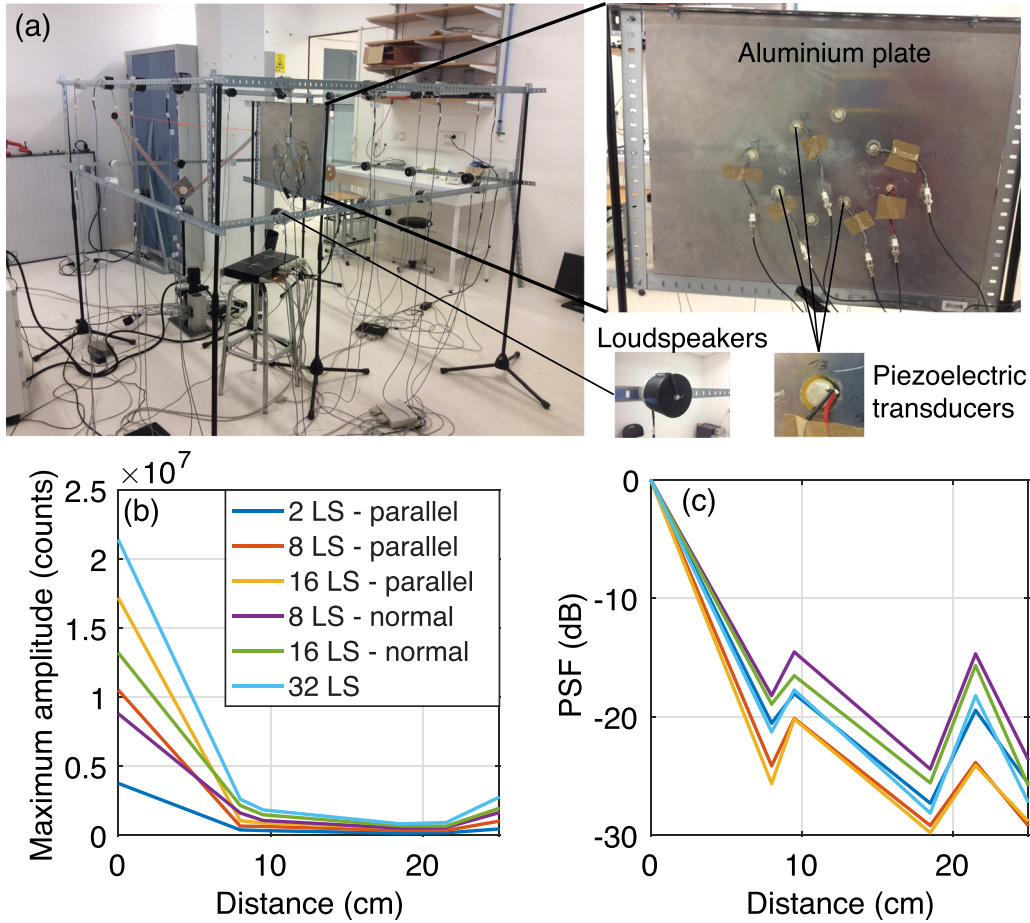
Farin *et al.*   2513

FIG. 3. (Color online) (a) Experimental setup to verify the effect of the geometry of the LS array on the focusing. Sixteen LS are in a plane parallel to the plate, and 16 are in a plane normal to the plate. The focusing is made in the plate at the position of a piezoelectric transducer, and the vibration amplitude is measured with five other piezoelectric transducers at various distances from the focal spot. (b) Maximum amplitude of vibration speed, and (c) PSF as a function of the distance from the focal spot.
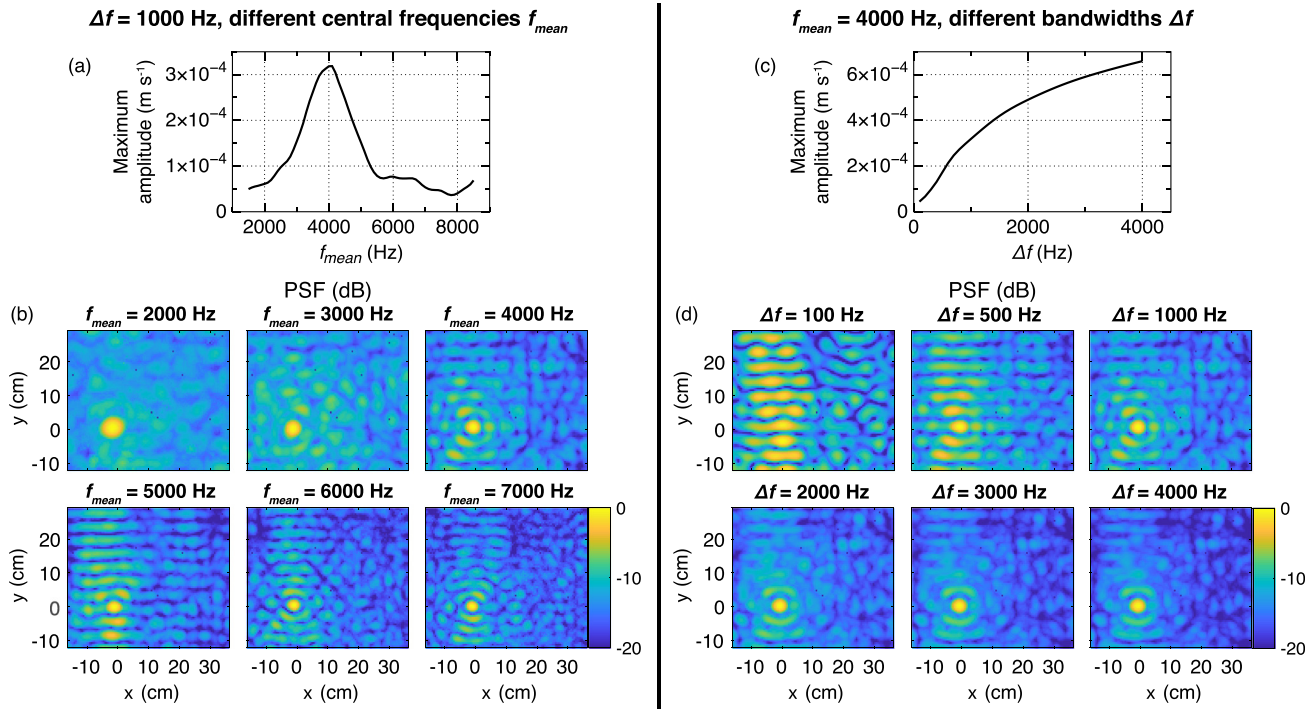

FIG. 4. (Color online) Influence of the central frequency and bandwidth of the sound excitation on the quality of the focusing on the large duralumin plate. (a)–(c) Maximum amplitudes of the focal spots, and (b)–(d) PSFs at positions (x,y) on the plate for different (a) and (b) central frequencies f_{mean}, and (c) and (d) bandwidths Δf. The focal spot is at position $(x=0, y=0)$.
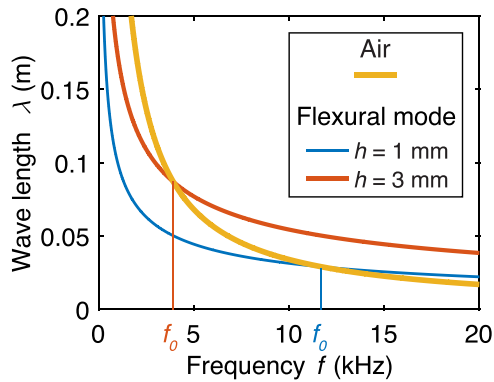
FIG. 5. (Color online) Wavelength λ of the flexural mode in thin duralumin plates of thickness $h = 1\,\mathrm{mm}$ and $h = 3\,\mathrm{mm}$ and acoustic wavelength in air. The critical frequency f_0 for which the flexural wavelength equals the air wavelength is indicated for both plates.

energy radiated in the plate over emitted acoustic energy) appears to be two times larger when the plate is placed inside the tube ($\cong 0.024\%$) than when the plate is alone ($\cong 0.011\%$; see Appendix A for details on the computations). This is a commonly observed effect of cavities (e.g., Ribay *et al.*, 2005; Willardson *et al.*, 2018; Yon *et al.*, 2003). The multiple acoustic wave reflections inside the tube increase the duration of the coda of the impulse response $k_i(t)$ compared to the case without the tube. The impulse response $k_i(t)$ may contain, therefore, more energy when the plate is inside the tube, thus the

amplitude of the plate excitation for a given emitted amplitude is higher. However, note that reverberation in the room where the experiment is conducted dominates the recorded coda with and without the tube. We further discuss the effect of room reverberation on our TR experiment in Sec. V.

B. Selective excitation

We now check selective excitation of a specific plate of a group of three placed inside the tube [Fig. 7(a)]. The plates are fixed in the tube by the way of slits. They are parallel to each other and separated by less than 1 cm. We first excite the plate opposite to the TRM [plate 1, Figs. 7(a) and 7(b)] and then the central plate (plate 2, Figs. 7(a) and 7(c)]. In both cases, the focal spot diameter is about 2 cm around position $(x = 0, y = 0)$. In addition, an amplitude ratio of about 5 (13 dB) is observed between the selected plate and its neighbors. Therefore, the selective excitation of a plate inside a complex structure is possible. Note that the focal spot on plate 2 [Fig. 7(c)] is slightly shifted from targeted position $(x = 0, y = 0)$ because we mainly excite one eigenmode of this plate.

V. DISCUSSION

A. DORT analysis

In order to provide a deeper understanding of focusing properties of the remote TR of flexural waves in a plate,
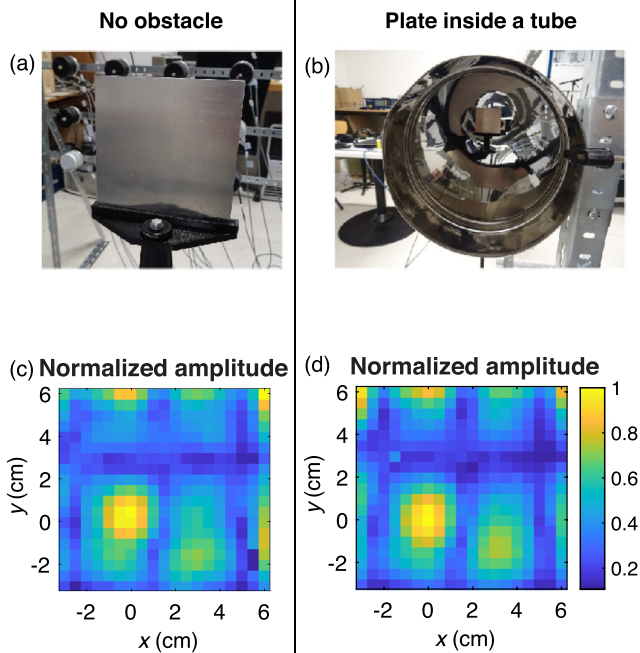

FIG. 6. (Color online) Comparison of the excitation of a small duralumin plate without and with a stainless steel tube around it. (a),(b) Pictures of the experiment. (c),(d) Normalized vibration speed amplitudes as a function of the positions on the small duralumin plate for (c) the plate alone and (d) the plate placed inside the tube. The focal spot is at position $(x = 0, y = 0)$. (e) Impulse recorded at the focal spot. (f) Enlargement around the impulse. (g) Amplitude spectrum of the signals in (e). The red signal is the noise level.

J. Acoust. Soc. Am. **146** (4), October 2019
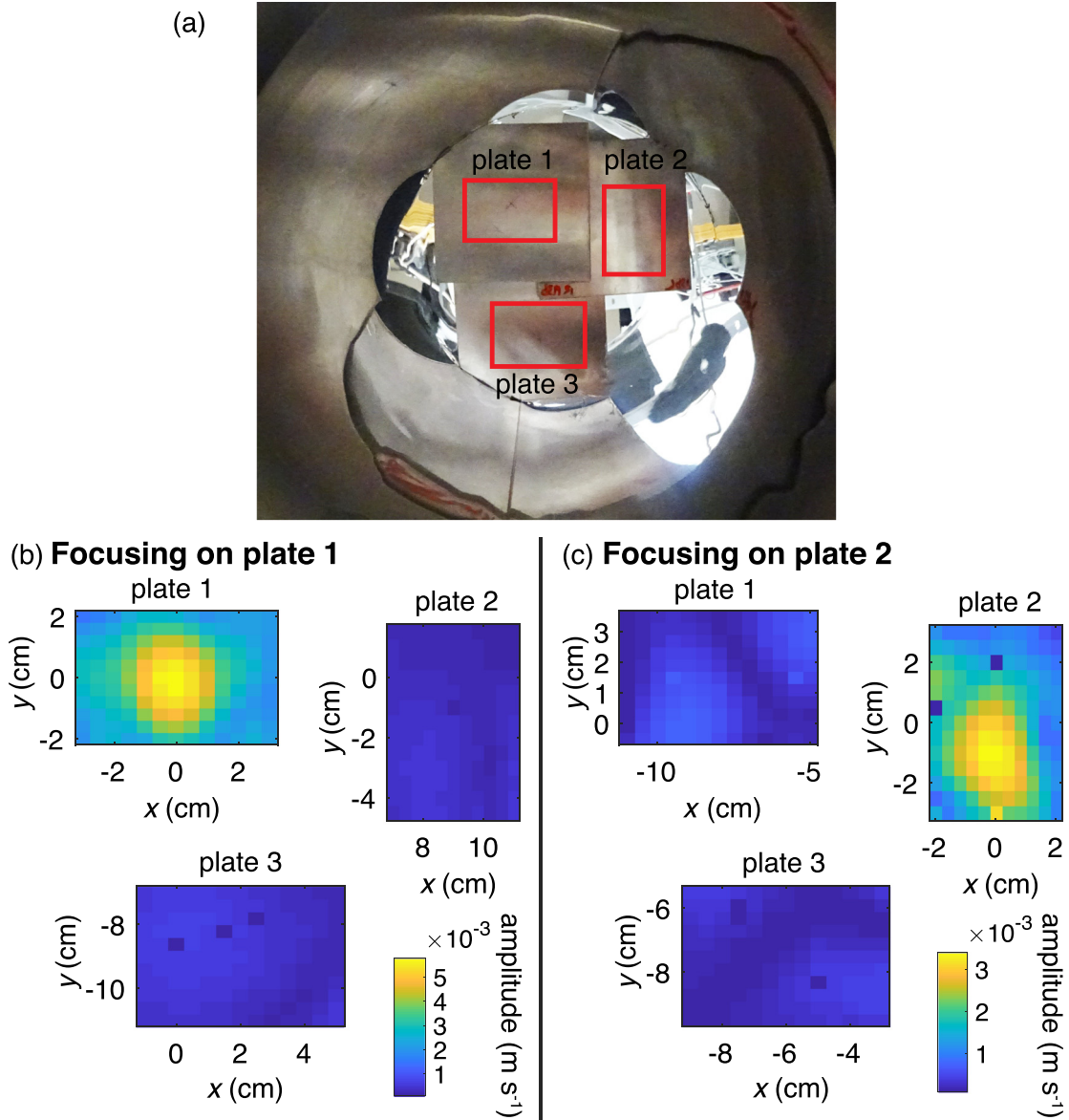
Farin *et al.* 2515
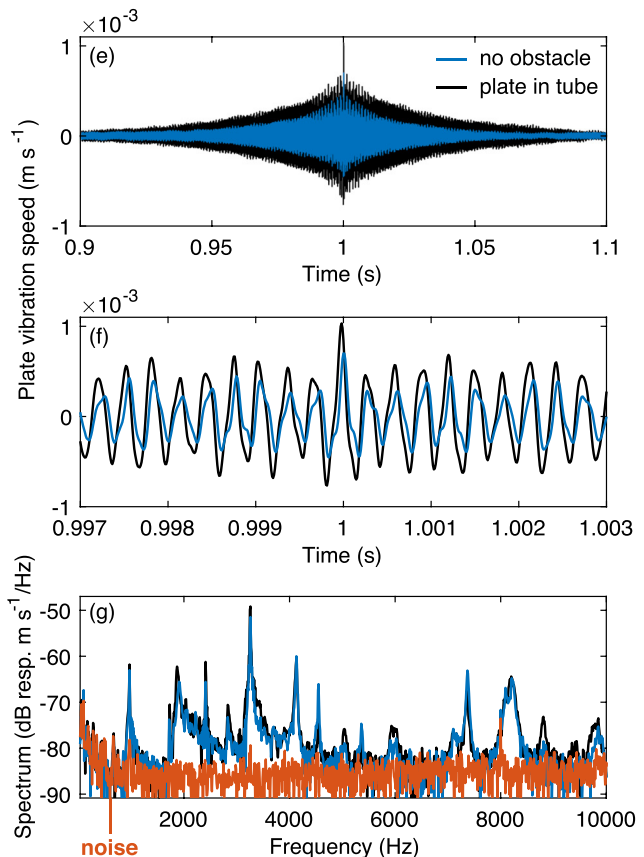
FIG. 7. (Color online) (a) Picture of the experimental setup of three small thin duralumin plates installed inside a tube. (b),(c) Maximum amplitude recorded on each plate inside the structure when the focal spot is on (b) plate 1 and (c) plate 2.

we perform a DORT analysis (French acronym for "decomposition of the time reversal operator"). The DORT method has been developed to go beyond the "basic" TR operation. The independent focusing wavefronts that can be generated by a TRM are evaluated from the diagonalization of the TR operator (e.g., Aubry *et al.*, 2001; Prada *et al.*, 1995; Prada *et al.*, 1996). For instance, in the case of two point-like reflectors that are well resolved and have different reflection coefficients, the DORT method provides the two waveforms that focus on each reflector. Usually, the DORT method is applied in a backscattering configuration, but here we use it to figure out the number and shape of the TR wavefronts between the TRM and the plate. The TR operator can be conveniently expressed in terms of the transfer matrix **K** such as $^{t}\mathbf{K}^{*}\mathbf{K}$. Note that superscript "t" and "$*$" stand for the transpose and conjugate operators, respectively. One element of the transfer matrix K_{ij} is the Fourier transform at a given frequency of f, the impulse response $k_{ij}(t)$. The eigenvectors

of the TR operator are the TR invariants: the waveform remains identical when they are time reversed. An efficient way to work out the eigenvectors is to perform the singular value decomposition (svd) of the transfer matrix $\mathbf{K}_{ij}$ for a given frequency ω_0,

$$\mathbf{K}_{ij}(\omega_0) = \sum_{n=1}^{N} \mathbf{U}_{jn}(\omega_0)\sigma_n(\omega_0)\mathbf{V}_{in}^{*}(\omega_0), \quad (2)$$

with N the number of LS (here, the number of positions scanned by the vibrometer is much larger than N), σ_n the singular values, and $\mathbf{U}_{jn}$ and $\mathbf{V}_{in}$ the singular vectors of $\mathbf{K}_{ij}$. The squared values σ_n^2 are equal to the eigenvalues of the TR operator. If we emit the time-reversed impulse responses with amplitude $\mathbf{V}_{in}$ with the LS at $\mathbf{r_i}$, we measure at $\mathbf{r_j}$ the wave field $\mathbf{U}_{jn}$ on the plate. The singular values σ_n for a given frequency $f = 4016\,\mathrm{Hz}$ are represented in Fig. 8(a). The highest singular value σ_1 as a function of the frequency allows us to identify the main eigenmodes of the
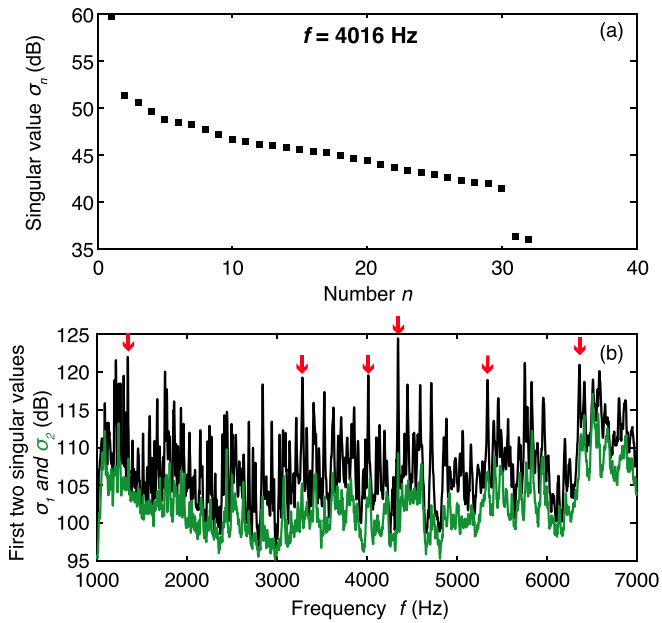
FIG. 8. (Color online) (a) Singular values σ_n for the mode of frequency $f = 4016$ Hz on the large duralumin plate. (b) First two highest singular values σ_1 (black) and σ_2 (green) as a function of frequency f. Arrows indicate some principal modes.

plate, which correspond to the peak values [Fig. 8(b)]. The field patterns $\mathbf{U}_{j1}$ of several eigenmodes identified in Fig. 8(b) and the associated vectors $\mathbf{V}_{i1}$ of amplitude that the LS emits to only excite these patterns are represented in Fig. 9.

At a resonance frequency, the first singular value σ_1 is about 10 dB higher than the second singular value σ_2 [Figs. 8(a) and 8(b)]. This is very different from the continuous singular value distribution at a given frequency, which is observed in previous studies dealing with open systems (e.g., Aubry *et al.*, 2001; Tanter *et al.*, 2000). In our case, only one field pattern can be generated on the plate at this frequency: the plate eigenmode. Thus, we need only a few LS to excite one plate eigenmode. As a consequence, the contrast of the focusing is not due to the plurality of LS, in agreement with what Draeger and Fink (1997) reported for one single channel TR. If one would like to excite a particular field pattern with only a few LS, one should preferentially place them at the spots corresponding to the higher values (darker color) of the singular vectors $\mathbf{V}_{i1}$. The values of $\mathbf{V}_{i1}$ are higher on the bottom row LS, which are just in front of the plate. As previously observed, this is consistent with the fact that the focusing amplitude does not increase linearly with the number of
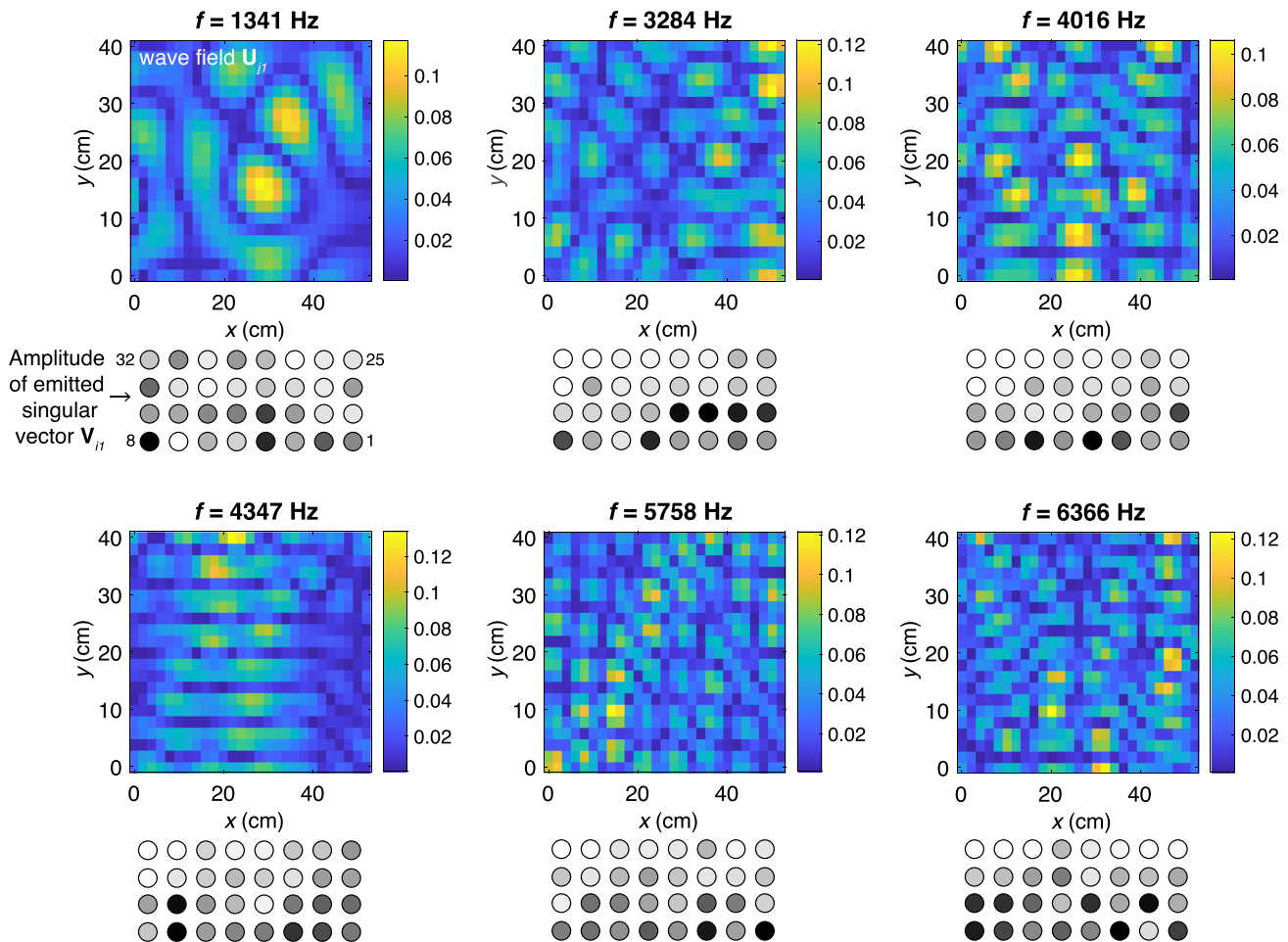

FIG. 9. (Color online) Normalized amplitude of the wave field $\mathbf{U}_{j1}(\omega)$ of different modes of the large duralumin plate (lighter colors represent higher amplitude) and amplitude $\mathbf{V}_{i1}(\omega)$ of the singular vectors that have to be emitted by the LS to obtain the corresponding wave field (black, maximum amplitude; white, minimal amplitude).

LS [Fig. 3(b)]. The fact that we only need a few LS to excite the plate eigenmodes explains why we observed that the secondary lobes level only slightly decreases from -18 dB to -20 dB when we use 8 LS instead of 2, and does not change when we use 16 LS instead of 8 in Fig. 3(c). With eight LS, we already efficiently excite all of the plate eigenmodes that interact constructively at the focal point, provided the bandwidth of the excitation signal is large enough. We do not excite more eigenmodes by using more LS. However, using more LS still improves the signal-to-noise ratio [Fig. 3(b)].

To sum up, the TR method is efficient to put in vibration a specific part of a complex structure which resonates for a given eigenmode. The svd of the transfer matrix $\mathbf{K}$ allows us to identify (i) the frequency of the eigenmode we would like to excite, (ii) the most appropriate positions for the elements of the TRM, and (iii) the signal the elements should emit to excite this specific eigenmode.

B. Influence of room reverberation

During routine health inspection in industries, one can imagine a TRM successively exciting the objects to control when they pass in front of it. Because the forward step is the longest step of the TR experiment, if one wants to gain time one may just record the impulse responses once for one object (forward step) and then emit these time-reversed impulse responses to excite the other objects when they are positioned at the same emplacement in front of the TRM (backward step). This procedure is similar to the one applied by Le Bas *et al.* (2015) to locally control the surface of a plate. However, this requires that the coda of the impulse responses are unchanged between the forward and backward steps, and therefore the cavity in which the TR process is performed does not change. Since we conducted our experiments in a room, we verify whether the impulse functions are strongly sensitive to sound reverberation in the room. To do so, we measure the
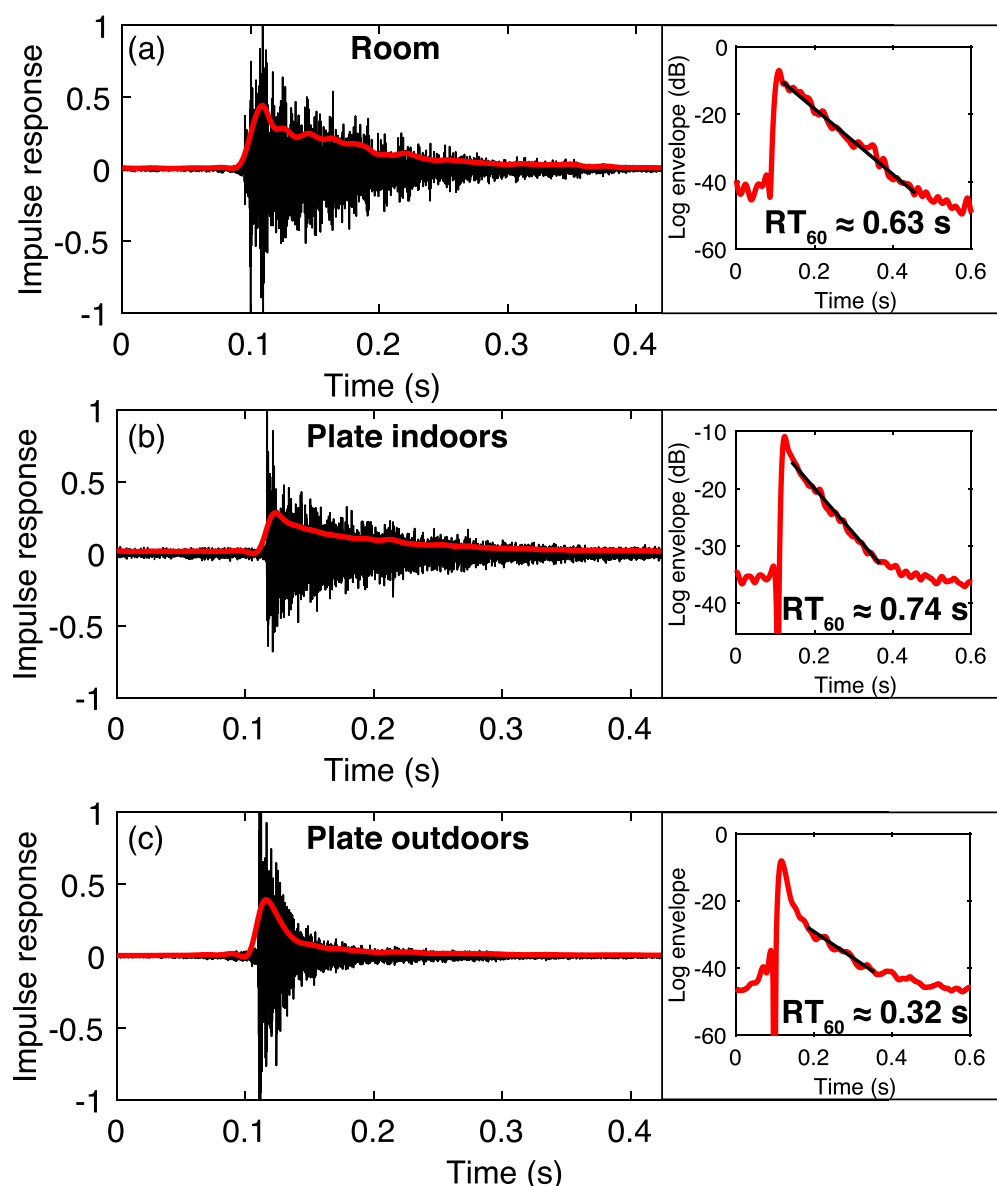

FIG. 10. (Color online) Impulse responses recorded between the TRM and (a) a microphone in the room, (b) the measurement position on the plate placed indoors, and (c) the measurement position on the plate placed outdoors. Red lines show the low-pass filtered envelopes below 100 Hz. (Insets) Logarithm of the envelop. The linear section of these curves indicates an exponential decay of the coda amplitude.

reverberation time, RT_{60}, necessary for the sound pressure to decrease by 60 dB for a wave path between the TRM and a microphone inside the room (room response) and between the TRM and the measurement position on the plate when it is placed inside the room (which includes room and plate response) or outdoors (without wall reflections). In the frequency range of interest (1–10 kHz), this time is $RT_{60} \cong 0.63$ s in the room, $RT_{60} \cong 0.74$ s on the plate indoors and $RT_{60} \cong 0.32$ s on the plate outdoors (Fig. 10). We note that the same experiment results in a reverberation time more than two times smaller when conducted outdoors instead of indoors. A significant part of the coda recorded on the plate indoors is therefore due to reverberation in the room. This is due to the fact that the plate is located at a distance from the TRM close to the critical distance for which the direct wave has the same amplitude as the reverberated sound in the room. We estimate that the critical distance in the room is about

$$d_c \cong 0.057 \sqrt{\frac{V}{RT_{60}}} \cong 0.77 \, \text{m} \tag{3}$$

with V the room volume (Peutz, 1971). Therefore, the impulse responses are sensitive to the environment (plate position, people, and furniture) in the room. Consequently, for future applications of our technique for health inspection, care must be taken to maximize the critical distance d_c (i.e., ratio V/RT_{60}) so that the impulse responses do not depend too much on environmental changes. In terms of the formalism used in Sec. V A, the fact that the room is reverberant principally affects the eigenvectors $\mathbf{V}_{i1}$. However, even though reverberation is important in the room, we still measure the eigenfrequencies of the plate, and that is what is important to conduct a health inspection.

VI. CONCLUSIONS

In this paper, remote spatial and temporal focusing of flexural waves in a thin plate was achieved using a TR technique in the audible frequency range (1–10 kHz). We showed that selective excitation of an object inside a complex structure is possible. The efficiency of the focusing (ratio of elastic energy radiated in the plate over emitted acoustic energy) is about 0.01%–0.02%. By computing the eigenvectors of the transfer matrix between the TRM and scanned points on the thin plate, we determined the signal to be emitted in order to excite specific eigenmodes of the plate. We observed that the level of secondary lobes of the focal spot does not decrease by using a large number of elements in the TRM because only one element is sufficient to excite an eigenmode. In contrast, the ratio of the amplitude at the focal spot over the amplitude of the secondary lobes increases when one increases the frequency bandwidth of the excitation signal because more eigenmodes are excited, and they interact constructively to form the focal spot. The presented technique could be useful to perform remote nondestructive control of difficultly to access plates within a complex structure. Note that several methods exist to enhance the amplitude of the focal spot during TR focusing (Willardson et al., 2018). Using these methods could be useful for future applications of the TR technique in structures with strong attenuation.

APPENDIX: DETERMINATION OF THE ACOUSTIC EFFICIENCY OF THE FOCUSING

The acoustic efficiency of flexural waves focusing in a thin plate is the ratio of the elastic energy E_{el} radiated in the plate over the acoustic energy E_{emit} emitted by the LS. Here, we detail the computations of the energies E_{emit} and E_{el}.

1. Energy emitted by the LS

One loudspeaker emits the acoustic pressure $p(r,t)$, function of distance r and time t. The acoustic power $\mathcal{P}(t)$ recorded at distance r from the loudspeaker is then

$$\mathcal{P}(t) = \frac{S}{Z_0} p(r,t)^2, \tag{A1}$$

with S the surface of the emitted wavefront at $r = 1$ m, and $Z_0 = \rho_0 c_0 \cong 413.5$ Pa s m^{-1} the air impedance, $\rho_0 \cong 1.2$ kg m^{-3} the air density, and $c_0 \cong 343$ m s^{-1} the sound speed in air at 20 °C. We assume the loudspeaker emits a hemispheric wavefront, thus, $S = 2\pi r^2$. The energy E_i emitted by the ith loudspeaker is then

$$E_i = \int_t \mathcal{P}(t) dt = \frac{2\pi r^2}{Z_0} \int_0^T p(r,t)^2 dt, \tag{A2}$$

with t_s the duration of the emitted signal. Practically, the acoustic pressure $p(r,t)$ is measured with a microphone placed at $r = 1$ m from the loudspeaker. The total energy emitted by all 32 LS is $E_{emit} = \sum_{i=1}^{32} E_i$.

2. Elastic energy radiated in the plate

The technique to determine the elastic energy radiated in the plate is based on the energy flux conservation through a surface surrounding the focal spot. The density of energy flux $\tilde{\Pi}(\omega)$, at cylindric frequency ω is, by definition, the bulk density of the total energy $\tilde{e}_{tot} = \tilde{e}_c + \tilde{e}_p$, integrated along the plate thickness h, multiplied by the energy speed, i.e., the group speed $v_g(\omega)$ (Royer and Dieulesaint, 2000)

$$\tilde{\Pi}(\omega) \hat{=} v_g(\omega) \int_{-h/2}^{h/2} \tilde{e}_{tot}(\omega) dz. \tag{A3}$$

For elastic waves propagating in a homogeneous guide, as a plate, the bulk density of kinetic and potential energies are equal

J. Acoust. Soc. Am. **146** (4), October 2019

Farin *et al.* 2519

$$\tilde{e}_c(\omega) = \tilde{e}_p(\omega) = \frac{1}{2}\rho_p|\tilde{V}_z(r,\omega)|^2, \qquad (A4)$$

with ρ_p the plate density and $\tilde{V}_z(r,\omega)$ the time Fourier transform of the vibration speed $v_z(r,t)$ measured at the plate surface. The elastic energy E_{el} radiated in the plate is given by the integral on the frequencies ω of the radiated power, which is the flux $\tilde{\Pi}(\omega)$ integrated along a line surrounding the focal spot

$$E_{el} = \frac{1}{2\pi}\int_{-\infty}^{+\infty}\left[\oint\tilde{\Pi}(\omega)r\mathrm{d}\theta\right]$$
$$= \frac{1}{2\pi}\int_{-\infty}^{+\infty}\left[v_g(\omega)\int\int_S\rho_p|\tilde{V}_z(r,\omega)|^2r\mathrm{d}\theta\mathrm{d}z\right]\mathrm{d}\omega. \qquad (A5)$$

At the focal spot, the vibration speed measured by the vibrometer can be written in the frequency domain

$$\tilde{V}_z(r,\omega) = \tilde{A}J_0(kr) = \frac{\tilde{A}}{2}\left(H_0^{(1)}(kr) - H_0^{(1)}(-kr)\right), \qquad (A6)$$

where $\tilde{A}$ is the maximum amplitude of the measured spectrum, J_0 is the Bessel function of the first kind, k is the wavenumber, and $H_0^{(1)}$ is the Hankel function of the first kind. $H_0^{(1)}(kr)$ represents the convergent wave, and $H_0^{(1)}(-kr)$ represents the divergent wave, which interfere with each other, and form the focusing impulse in $kr = 0$. We only consider the convergent wave. If we integrate over a sufficiently large surface (for large r), we can develop the Hankel function in far field and write the vibration speed as

$$\tilde{V}_z(r,\omega) \cong \frac{\tilde{A}}{2}H_0^{(1)}(kr) \cong \frac{\tilde{A}}{2}\sqrt{\frac{2}{\pi kr}}e^{-jkr}. \qquad (A7)$$

By replacing $\tilde{V}_z(r,\omega)$ in Eq. (A5), we obtain

$$E_{el} \cong \frac{1}{2\pi}\rho_p h\int_{-\infty}^{+\infty}\tilde{A}^2\frac{v_g(\omega)}{k(\omega)}\mathrm{d}\omega. \qquad (A8)$$

In a plate, for the flexural mode, the group speed $v_g(\omega) = 2\omega/k(\omega)$ and the dispersion relation is $k(\omega)^2 = \sqrt{\rho_p h/D}\omega$, with D the flexural stiffness of the plate (Royer and Dieulesaint, 2000). Then, $v_g(\omega)/k(\omega)$ simplifies and becomes $\sqrt{D/(\rho_p h)}$ (independent of ω). Thus,

$$E_{el} \cong \frac{1}{2\pi}\sqrt{\rho_p h D}\int_{-\infty}^{+\infty}\tilde{A}^2\mathrm{d}\omega, \qquad (A9)$$

that can be expressed in the frequency domain, according to Parceval theorem,

$$E_{el} \cong \frac{1}{2\pi}\sqrt{\rho_p h D}\int_0^{\Delta t}A^2\mathrm{d}t, \qquad (A10)$$

with A the maximum amplitude of the measured impulsion $v_z(r,t)$ at the focal spot, and Δt the impulsion duration.

Anderson, B., Remillieux, M., Le Bas, P.-Y., and Ulrich, T. (**2019**). *Time Reversal Techniques. Nonlinear Ultrasonic and Vibro-Acoustical Techniques for Nondestructive Evaluation* (Springer, Berlin), pp. 547–581.

Aubry, J.-F., Tanter, M., Gerber, J., Thomas, J.-L., and Fink, M. (**2001**). "Optimal focusing by spatio-temporal inverse filter. II. Experiments. Application to focusing through absorbing and reverberating media," J. Acoust. Soc. Am. **110**, 48–58.

Chakroun, N., Fink, M., and Wu, F. (**1995**). "Time reversal processing in ultrasonic nondestructive testing," IEEE Trans. Ultrason. Ferroelectr. Freq. Control **42**, 1087–1098.

Derode, A., Roux, P., and Fink, M. (**1995**). "Robust acoustic time reversal with high-order multiple scattering," Phys. Rev. Lett. **75**(23), 4207–4209.

Diamanti, K., and Soutis, C. (**2010**). "Structural health monitoring techniques for aircraft composite structures," Prog. Aerosp. Sci. **46**, 342–352.

Draeger, C., Aime, J., and Fink, M. (**1998a**). "One-channel time-reversal in a chaotic cavities: Experimental results," J. Acoust. Soc. Am. **105**(2), 618–625.

Draeger, C., Cassereau, D., and Fink, M. (**1998b**). "Acoustic time reversal with mode conversion at a solid-fluid interface," Appl. Phys. Lett. **72**, 1567–1569.

Draeger, C., and Fink, M. (**1997**). "One-channel time reversal of elastic waves in a chaotic 2D-silicon cavity," Phys. Rev. Lett. **79**(3), 407–410.

Etaix, N., Dubois, J., Fink, M., and Ing, R.-K. (**2013**). "Increasing the modal density in plates for mono-element focusing in air," J. Acoust. Soc. Am. **134**, 1049–1054.

Etaix, N., Fink, M., and Ing, R.-K. (**2012**). "Acoustic imaging device with one transducer," J. Acoust. Soc. Am. **131**, EL395.

Filippi, P. (**2010**). *Vibrations and Acoustic Radiation of Thin Structures: Physical Basis, Theoretical Analysis and Numerical Methods* (Wiley, Hoboken, NJ).

Fink, M., Cassereau, D., Derode, A., Prada, C., Roux, P., Tanter, M., Thomas, J.-L., and Wu, F. (**2000**). "Time-reversed acoustics," Rep. Prog. Phys. **63**, 1933–1995.

Ing, K., and Fink, M. (**1998**). "Time-reversed Lamb waves," IEEE Trans. Ultrason. Ferroelectr. Freq. Control. **45**, 1032–1043.

Kuperman, W., Hodgkiss, W., Song, H., Akal, T., Ferla, C., and Jackson, D. (**1998**). "Phase conjugation in the ocean: Experimental demonstration of an acoustic time-reversal mirror," J. Acoust. Soc. Am. **103**, 25–40.

Le Bas, P.-Y., Remillieux, M., Pieczonka, L., Ten Cate, J., Anderson, B., and Ulrich, T. (**2015**). "Damage imaging in a laminated composite plate using an air-coupled time reversal mirror," Appl. Phys. Lett. **107**, 184102.

Le Bas, P.-Y., Ulrich, T., Anderson, B., and Esplin, J. (**2013**). "A high amplitude, time reversal acoustic non-contact excitation (trance)," J. Acoust. Soc. Am. **134**, EL52.

Montaldo, G., Roux, P., Derode, A., Negreira, C., and Fink, M. (**2001**). "Generation of very high pressure pulses with 1-bit time reversal in a solid waveguide," J. Acoust. Soc. Am. **110**, 2849–2857.

Payan, C., Remillieux, M., Le Bas, P.-Y., Ulrich, T., Massacret, N., and Moysan, J. (**2017**). "Selective mode focusing in a plate of arbitrary shape applying time reversal mirrors," Acta Acust. **103**, 950–953.

Peutz, V. (**1971**). "Articulation loss of consonants as a criterion for speech transmission in a room," J. Audio Eng. Soc. **19**(11), 915–919, available at http://www.aes.org/e-lib/browse.cfm?elib=2108.

Prada, C., Manneville, S., Spoliansky, D., and Fink, M. (**1996**). "Decomposition of the time reversal operator: Detection and selective focusing on two scatterers," J. Acoust. Soc. Am. **99**, 2067–2076.

Prada, C., Thomas, J.-L., and Fink, M. (**1995**). "The iterative time reversal process: Analysis of the convergence," J. Acoust. Soc. Am. **97**, 62–71.

Quieffin, N., Catheline, S., Ing, R., and Fink, M. (**2004**). "Real-time focusing using an ultrasonic one channel time-reversal mirror coupled to a solid cavity," J. Acoust. Soc. Am. **115**, 1955–1960.

Ribay, G., de Rosny, J., and Fink, M. (**2005**). "Time-reversal of noise sources in a reverberation room," J. Acoust. Soc. Am. **117**, 2866–2872.

Rivière, J., Renaud, G., Haupert, S., Talmant, M., Laugier, P., and Johnson, P. (**2010**). "Nonlinear acoustic resonances to probe a threaded interface," J. Appl. Phys. **107**, 124901.

Royer, D., and Dieulesaint, E. (**2000**). *Elastic Waves in Solids I: Free and Guided Propagation* (Springer, Berlin).

Salawu, O. (**1997**). "Detection of structural damage through changes in frequency: A review," Eng. Struct. **19**, 718–723.

Tanter, M., Thomas, J., and Fink, M. (**2000**). "Time reversal and the inverse filter," J. Acoust. Soc. Am. **108**, 223–234.

Van Den Abeele, K., Van Damme, B., and Delrue, S. (**2010**). "Application of the chaotic cavity transducer concept for imaging in non-reverberant media," J. Acoust. Soc. Am. **127**, 1947.

Wallace, C. (**1972**). "Radiation resistance of a rectangular panel," J. Acoust. Soc. Am. **51**, 946–952.

Willardson, M., Anderson, B., Young, S., Denison, M., and Patchett, B. (**2018**). "Time reversal focusing of high amplitude sound in a reverberation chamber," J. Acoust. Soc. Am. **143**(2), 696–705.

Yon, S., Tanter, M., and Fink, M. (**2003**). "Sound focusing in rooms: The time-reversal approach," J. Acoust. Soc. Am. **113**(3), 1533–1543.